Structures of Tetrasilylmethane Derivatives $C(SiXMe_2)_4$ (X = H, F, Cl, Br) in the Gas Phase and their Dynamic Structures in Solution

Derek A. Wann[a], Stuart Young[a], Karin Bätz[b], Sarah L. Masters[c], Anthony G. Avent[d,†], David W. H. Rankin[e], and Paul D. Lickiss[b]

[a] Department of Chemistry, University of York, Heslington, York, UK YO10 5DD
[b] Department of Chemistry, Imperial College London, London, UK SW7 2AZ
[c] Department of Chemistry, University of Canterbury, Private Bag 4800, Christchurch 8140, New Zealand
[d] Department of Chemistry, School of Life Sciences, University of Sussex, Falmer, Brighton, UK BN1 9QJ
[e] School of Chemistry, University of Edinburgh, West Mains Road, Edinburgh, UK EH9 3JJ
[†] Deceased

Reprint requests to Dr. D. A. Wann. E-mail: derek.wann@york.ac.uk

Z. Naturforsch. **2014**, *69b*, 1321 – 1332 / DOI: 10.5560/ZNB.2014-4147
Received July 8, 2014

Dedicated to Professor Hubert Schmidbaur on the occasion of his 80th birthday

The structures of the molecules $C(SiXMe_2)_4$ (X = H, F, Cl, Br) have been determined by gas electron diffraction (GED). *Ab initio* calculations revealed nine potential minima for each species, with significant ranges of energies. For the H, F, Cl, and Br derivatives nine, seven, two, and two conformers were modelled, respectively, as they were quantum-chemically predicted to be present in measurable quantities. Variable-temperature ^{1}H and ^{29}Si solution-phase NMR studies and, where applicable, ^{13}C NMR, ^{1}H/^{29}Si NMR shift-correlation, and ^{1}H NMR saturation-transfer experiments are reported for $C(SiXMe_2)_4$ (X = H, Cl, Br, and also I). At low temperature in solution two conformers (one C_1-symmetric and one C_2-symmetric) are observed for each of $C(SiXMe_2)_4$ (X = Cl, Br, I), in agreement with the isolated molecule *ab initio* calculations carried out as part of this work for X = Cl, Br. $C(SiHMe_2)_4$ is present as a single C_1-symmetric conformer in solution at the temperatures at which the NMR experiments were performed.

Key words: Silyl Methane Derivatives, Gas Electron Diffraction, Variable-Temperature NMR

Introduction

The chemistry of tetrasilylmethane derivatives has been studied extensively, with the severe steric constraints imposed by four Si-centred substituents attached to a carbon atom often leading to unusual reactivities and novel structural features [1 – 4]. The most widely studied tetrasilylmethane derivatives have the general structures $(Me_3Si)_3CSiRR'X$, $(PhMe_2Si)_3CSiRR'X$, and $(Me_3Si)_2C(SiXMe_2)(SiR_2Y)$ (where R and R′ = Me, Et, Ph *etc.* and X, Y = H, halide, OAc *etc.*) [1 – 4].

A range of related tetrasilylmethanes with four substituents of the same kind $C(SiXMe_2)_4$ (X = H [5 – 8], Ph [9 – 11], OH [12, 13], OMe [6, 14], OEt [6, 14], OAc [6], O_2CCF_3 [6], OSO_2CF_3 [15], OSO_2-C_6H_4-*p*-Me [15], F [6], Cl [6, 16, 17], Br [6], and I [6] are known, although little of their chemistry has been explored. In contrast, the permethyl species, $C(SiMe_3)_4$, has been the subject of numerous reports, using NMR spectroscopy [18 – 22], X-ray diffraction [23 – 25], gas electron diffraction (GED) [26, 27], quantum-chemical calculations [28, 29], and vibrational spectroscopy [29].

Dynamic processes in bulky tetrasilylmethane derivatives have been studied previously by NMR spectroscopy in solution, for example, for $C(SiMe_3)_2(SiMePh_2)(SiMe_2ONO_2)$ [30], $C(SiMe_3)_2(SiClPh_2)(SiMe_2OMe)$ [31], and $(Me_3Si)_3CSiX_3$ (X = Cl, Br) and $(PhMe_2Si)_3SiCl_3$ [32]. $(Me_3Si)_3CSiH_3$ was stud-

ied using both NMR spectroscopy and GED [33], while GED studies have also been carried out for $(Me_3Si)_3CSiCl_3$ [34], and for $(HMe_2Si)_3CSiH_3$ [35], which showed the presence of eleven distinct conformers.

The work presented here comprises two main parts. First, the multiconformer structures of $C(SiXMe_2)_4$ [X = H (**1**), F (**2**), Cl (**3**), Br (**4**)] have been determined by GED experiments aided by *ab initio* calculations. Secondly, an NMR spectroscopic investigation of the dynamic processes occurring in $C(SiXMe_2)_4$ species [this time including X = I (**5**)] in solution has been undertaken.

Experimental Section

Syntheses of $C(SiXMe_2)_4$ (X = H, F, Cl, Br, I)

The syntheses of $C(SiHMe_2)_4$ (**1**) [5, 6], $C(SiFMe_2)_4$ (**2**) [6], $C(SiClMe_2)_4$ (**3**) [6], $C(SiBrMe_2)_4$ (**4**) [6], and $C(SiIMe_2)_4$ (**5**) [6] were carried out using methods previously reported in the literature, and outlined in Scheme 1. Yields were generally good, and the compounds were purified by sublimation.

NMR spectroscopy

The ^1H, ^{13}C, and ^{29}Si NMR spectra were recorded in $CDCl_3/CD_2Cl_2$ or $CDCl_3/[D_6]$acetone solutions using a Bruker AMX 500 spectrometer at 500, 126, and 99 MHz, respectively, unless otherwise stated. The $^{29}Si\{^1H\}$ NMR INEPT spectra were recorded using a Bruker AMX 500 NMR spectrometer at 99 MHz, while $^{29}Si\{^1H\}$ inverse-gated NMR spectra were recorded on a Bruker Avance 600 spectrometer at 119.23 MHz. Chemical shifts for all NMR spectra are reported in ppm relative to TMS.

Computational methods

With four $SiXMe_2$ groups present in each of **1**–**4**, rotation about the C(1)–Si(2/3/4/5) bonds allows many possible conformers to exist. The atom numbering used throughout this work is shown in Fig. 1. Before interpreting gas electron diffraction data it is important to identify all possible minimum-energy structures and compare their energies, to judge which will be present in observable amounts at the experimental conditions. Experience suggests that molecules such as **1**–**4** often have groups that are rotated by 15 – 20° from a perfectly staggered geometry, and that +20° and −20° for any particular group may give different structures, depending on the overall symmetry [36]. The four $SiXMe_2$ groups for each of **1**–**4** were treated as two pairs [the groups based on Si(2) and Si(3) were defined relative to one another and, similarly the groups based on Si(4) and Si(5) were paired], allowing dihedral angles to be uniquely defined as X(14)–Si(2)–C(1)–Si(3), X(16)–Si(3)–C(1)–Si(2), X(15)–Si(4)–C(1)–Si(5), and X(17)–Si(5)–C(1)–Si(4). Allowing just one of the $SiXMe_2$ groups to rotate with all others fixed, a potential-energy scan was performed; this indicated that each group could be present in three possible minimum-energy orientations, with dihedral angles (as defined above) of approximately −80, 160, and 40°. With four $SiXMe_2$ groups acting independently that gives a total of 3^4 (= 81) possible conformations. Considering the negative sense of each dihedral angle (*i. e.* 80, −160 and –40°) gives an additional 81 possible conformers.

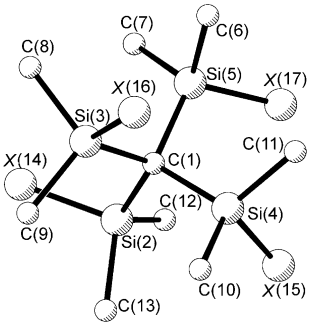

Fig. 1. Representation of the general structure of $C(SiXMe_2)_4$ with atom numbering. Hydrogen atoms have been removed for clarity. For numbering of subsequent conformers, $[41 \times (n-1)]$ should be added, where n is the number of the conformer.

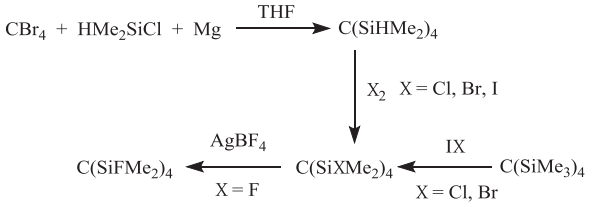

Scheme 1. Synthetic routes to $C(SiXMe_2)_4$ (X = H, F, Cl, Br, I) compounds.

Geometry optimisations and frequency calculations were carried out to determine the free energies of all conformers. All calculations utilised the GAUSSIAN 09 [37] suite of programs and were performed on the University of Edinburgh ECDF cluster [38] or the UK National Service for Computational Chemistry Software clusters [39]. For comparison, both the B3LYP [40 – 42] and M06-2X [43] methods with 6-31G(d) basis sets [44, 45] were used for these calculations.

For each species nine low-energy conformers were identified, and further geometry optimisations and frequency calculations were then carried out. The B3LYP hybrid method

with the aug-cc-pVDZ basis set [46, 47] was used for most atom types, with the aug-cc-pVDZ-PP [48, 49] pseudopotential basis set used for the heavy bromine atoms in **4**. Calculations were also performed using the M06-2X and MP2 methods [50] with the aug-cc-pVDZ(-PP) basis sets. All MP2 calculations were performed with a frozen core.

For each of **1**–**4**, force fields were calculated using analytic second derivatives of the energy with respect to the nuclear coordinates obtained at the M06-2X/aug-cc-pVDZ(-PP) level. These were then used with the program SHRINK [51, 52] to provide estimates of the amplitudes of vibration (u_{h1}) and curvilinear vibrational correction factors (k_{h1}) to internuclear distances required for the GED refinements.

Gas electron diffraction (GED)

The GED data used for the refinements of each of $C(SiXMe_2)_4$ (X = H, F, Cl, Br) (**1**–**4**) were collected using the apparatus formerly housed in Edinburgh [53], from samples that were synthesised and characterised at Imperial College London. Scattering intensities were recorded on Kodak Electron Image film at two nozzle-to-film distances, maximising the scattering angles over which data were collected. All nozzle-to-film distances and sample and nozzle temperatures are given in Table S1 in the Supporting Information available online (see note at the end of the paper for availability).

The photographic films were scanned using an Epson Expression 1680 Pro flatbed scanner using a routine method described elsewhere [54]. The data reduction and least-squares processes were carried out using the ED@ED v3.0 program [55], with the scattering factors of Ross *et al.* [56].

X-Ray crystallography

Several attempts were made to carry out single-crystal X-ray diffraction structural analyses of $C(SiHMe_2)_4$ (**1**), $C(SiClMe_2)_4$ (**3**) and $C(SiBrMe_2)_4$ (**4**) using an OD Xcalibur 3 diffractometer at 100 K in order to freeze out any dynamic disorder. Single crystals of **1** proved difficult to grow and, although the material diffracted, the quality of the diffraction pattern obtained was too poor to yield a believable unit cell. However, a highly symmetrical space group was suspected based on the behaviour of the crystals under polarised light. Both **3** and **4** were found to belong to the cubic space group $Pa\bar{3}$, with unit-cell dimensions of 12.46 and 12.53 Å, respectively. This space group requires complete disorder of chlorine and bromine positions along with at least two different sets of silicon positions. The disorder present precluded the identification of any specific conformers, and no model structures could be obtained for either **3** or **4**. A similar problem was noted previously for $C(SiIMe_2)_4$, which also crystallised in a cubic unit cell [$a = 12.982(1)$ Å] [57].

Results and Discussion

Gas-phase static structures

Nine conformers were identified for each of **1**–**4**, arising from geometry optimisations started from all possible combinations of dihedral angle minima. Using the Boltzmann equation and the Gibbs free energy for each conformer, the relative amounts of all conformers were determined at the temperatures of the experiments. As is common practice, and to maintain the data-to-parameter ratios, only conformers present with more than approximately 5 % abundance were included in the model for refinement.

As an example, the free energies of all nine conformers of $C(SiBrMe_2)_4$ (**4**) are listed in Table 1. Similar listings of energies for $C(SiXMe_2)_4$ (X = H, F, Cl) are given in Tables S2 – 4, respectively. Also shown are the relative amounts of each conformer that would be present in the GED samples at the temperature of that experiment. Because of the large energy differences between the conformers, only two of the nine possible conformers of **4** would likely be observed in the GED experiment; these have been designated conformer 1 (C_1 symmetry), and conformer 2 (C_2 symmetry). The molecular structure and numbering of $C(SiBrMe_2)_4$ can be seen in Fig. 1. The atomic numbering scheme is the same for all four species (**1**–**4**) studied using GED.

Table 1. Total free energies and energy differences between conformers of $C(SiBrMe_2)_4$ (**4**) calculated at the M06-2X/6-31G(d) level.

Conformer[a]	Symmetry	Total free energy (kJ mol^{-1})	Relative energy[b] (kJ mol^{-1})	Abundance[c] (%)
1	C_1	−8336788.25	0.00	75.5
2	C_2	−8336785.25	3.01	16.7
3*	C_1	−8336775.50	12.78	2.4
4*	C_1	−8336774.36	13.92	1.8
5*	C_1	−8336774.32	13.97	1.7
6*	C_2	−8336775.77	12.51	1.3
7*	D_2	−8336774.09	14.20	0.4
8*	C_1	−8336765.55	22.76	0.2
9*	C_2	−8336761.61	26.71	0.0

[a] Conformers marked with a star were not considered to be present in sufficient quantities to be included in the GED refinement model; [b] energy differences are relative to conformer 1, the lowest-energy conformer; [c] calculated at the average temperature of the GED experiment.

GED studies

Experimental GED data were refined using parameterised models based on bond lengths, bond angles, and dihedral angles, guided by calculations at the MP2/aug-cc-pVDZ(-PP) level. The following description is for the Br derivative (**4**), but all models are based upon similar sets of bond lengths and angles, with the only significant differences being additional dihedral angle parameters arising from the number of conformers being modelled. Each species is described by four distances, ten bond angles, and two dihedral angles. Full lists of parameters for each of **1**–**4** (Tables S5–S8) and the model descriptions can be found in the Supporting Information.

From geometry optimisations it was observed that the four $SiXMe_2$ groups exist in a near tetrahedral geometry, with only slight deviations from the ideal tetrahedral angles. These deviations, as well as many other small deviations related to parameters used in the models, are taken into account using fixed (non-refinable) differences in the models. Fixed differences were also used to define small variations between the principal conformer for each species and any higher-energy conformers.

On the basis of the data presented in Table 1 and in Tables S2 – 4, the models were written to fit nine, seven, two, and two conformers for the H, F, Cl, and Br derivatives, respectively. For each of these species the differences between conformers were shown by MP2/aug-cc-pVDZ(-PP) calculations to be small. The approach taken when writing the models was, therefore, to choose parameters that adequately described the dominant conformer, and then to use fixed differences to describe the minor conformers.

The SARACEN [58 – 60] method was used for the refinement of experimental data, with the required restraints based upon comparison of calculations at the MP2, B3LYP and M06-2X levels of theory, and with 6-31G(d) and aug-cc-pVDZ basis sets (using aug-cc-pVDZ-PP as a pseudopotential for Br in **4**). Vibrational corrections were based upon data from SHRINK [51, 52], calculated using force constants obtained from GAUSSIAN.

As is common, because they are not particularly well defined from the GED data, restraints were placed upon the distance difference parameters, as well as upon parameters associated with hydrogen atoms. Many dihedral angles were also restrained during the refinement process.

Amplitudes of vibration were grouped together, excluding those involving hydrogen, under their respective peaks in the radial distribution curves, with only that with the greatest scattering intensity refining. Other amplitudes under a given peak were allowed to change according to their ratios with respect to the refining value. Eleven amplitudes were refined for the Br derivative. Full lists of interatomic distances and amplitudes of vibration for **1**–**4** can be found in Tables S9 – 12, respectively.

All refinements were initially performed with the proportion of each conformer fixed at predicted values. For species **4** the proportion of conformer 1 was then stepped in increments of 0.05 either side of the predicted amount and the *R* factor recorded to ascertain the best fit. Fig. 2 shows this for **4**, where the 95 % confidence limit is also marked to allow the uncertainty in this measurement to be estimated [61]. The final proportion of conformer 1 was almost identical to that calculated, giving some reassurance that the Gibbs free energies were accurate. For **1**–**3** such an experimental determination was not possible. For **1** and **2** the presence of very many conformers with similar energies means that a satisfactory way of fixing some proportions and varying others could not be achieved. For **3** the quality of the experimental data are relatively poor (see further discussion later), and varying the amount of conformer 1 resulted in the *R* factor being lowest

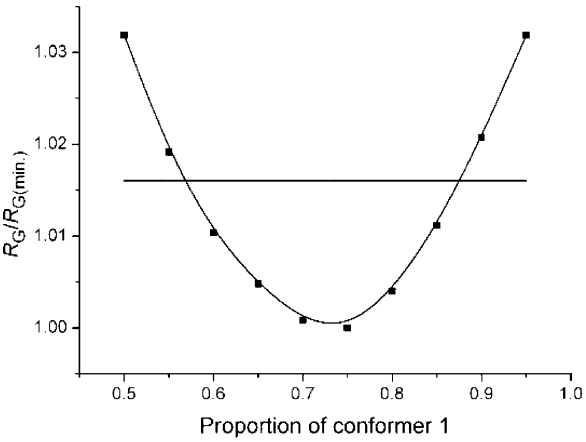

Fig. 2. Variation in R_G/R_G(min.) with different amounts of conformer 1 for species **4**. The horizontal line denotes the 95 % confidence limit, approximately equal to 2 σ.

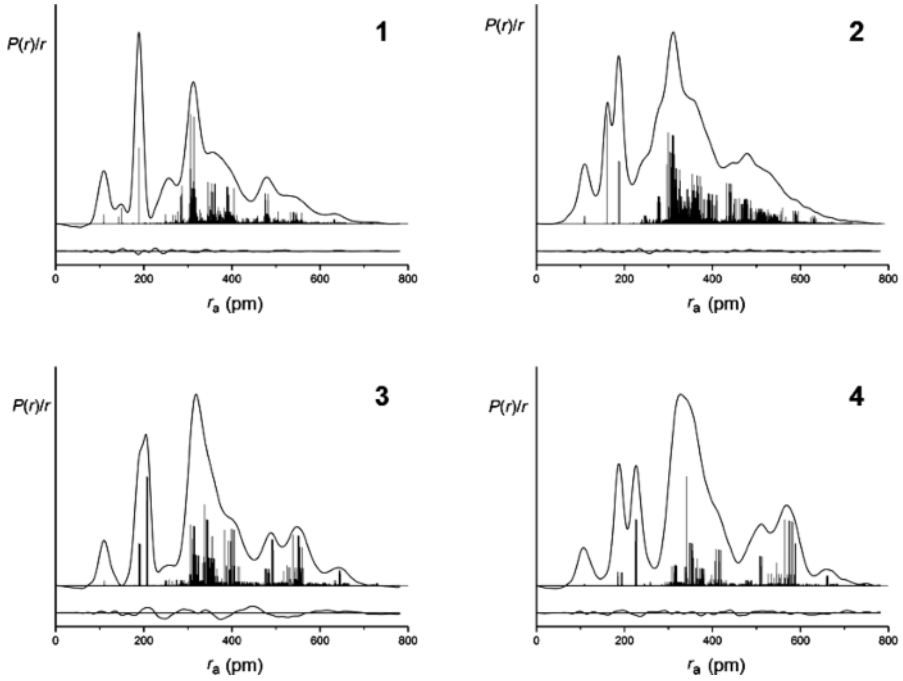

Fig. 3. Experimental and difference (experimental-minus-theoretical) radial distribution curves, $P(r)/r$, from the GED refinement of $C(SiXMe_2)_4$ [X = H (**1**), F (**2**), Cl (**3**), Br (**4**)]. Before Fourier inversion, data for **1** and **2** were multiplied by $s\cdot\exp(-0.00002s^2)/(Z_C - f_C)(Z_{Si} - f_{Si})$, while data for **3** and **4** were multiplied by $s\cdot\exp(-0.00002s^2)/(Z_C - f_C)(Z_X - f_X)$.

when the proportion of conformer 1 was 1.0; we do not believe that this is a realistic estimate.

Experimental radial distribution curves and difference curves can be seen for all four species in Fig. 3, illustrating the goodness of fits to the respective GED data. The R_G values obtained for X = H, F, Cl, Br were 8.4, 12.2, 11.0, and 12.5 %, respectively, with R_D values (ignoring off-diagonal elements of the weight matrix) of 7.5, 5.1, 10.0, and 7.5 %, respectively. A more complete explanation of differences between R_G and R_D can be found in ref. [62]. Figs. S1 – 4 show the related molecular intensity scattering curves as well as enlarged versions of the radial distribution curves in Fig. 3. Tables S13 – 16 show the correlation matrices for the refinements of each of **1** to **4**, while Tables S17 – 20 give the refined atomic positions of all conformers for the four species studied, and Tables S21 – 24 the equivalent calculated coordinates.

As mentioned earlier, a visual inspection of radial distribution curves for **3** indicates that the data were rather noisy. However, the R_G factor for the refinement of **3** suggests that these data fit at least as well as is the case for **2** and **4**. We can conclude that there was something affecting the quality of the raw data in the case of **3**, though we don't believe that this significantly affected the quality of the refinement.

Selected refined and calculated parameters for **1**–**4** are given in Tables 2 – 5. The bond lengths and angles shown correspond to the most abundant conformer of each species as this was the basis for the models, while dihedral angles describing the relative positions of the $SiXMe_2$ groups for all conformers are shown as these are individual to each conformer. Although each conformer can have two (C_2 symmetry) or four (C_1 symmetry) different C(1)–Si distances for each conformer of each of **1**–**4**, the variation in the C(1)–Si distances is small, with ranges of no more than 1 pm for a given species. Only one distance of this type is therefore shown in each of Tables 2 – 5.

For **1**, agreement between calculations and experimental data is seen for all bonded distances. Calculations at the B3LYP level (see Table 2) show a consistent overestimation of distances in the molecule, although the angles obtained are within 0.3° of the experimental values. Both MP2 and M06-2X level calculations for **1** give closer agreement to experimental data

Table 2. Selected experimental (r_{h1}) and quantum-chemically calculated (r_e) geometric parameters for **1**[a].

Parameter	r_{h1}	r_e B3LYP	r_e M06-2X	r_e MP2
*r*C(1)–Si(2)	189.4(4)	192.4	189.9	191.2
*r*Si(2)–C(12)	189.2(2)	189.9	188.9	189.9
*r*Si(2)–H(14)	149.9(8)	150.1	149.9	150.2
∠Si(2)–C(1)–Si(3)	108.3(1)	107.8	108.1	108.1
∠C(1)–Si(2)–C(12)	114.2(3)	114.1	113.2	113.3
∠C(1)–Si(2)–C(13)	114.2(3)	114.3	112.9	113.1
∠C(1)–Si(2)–H(14)	107.6(4)	107.4	108.0	107.8
∠C(10)–Si(4)–C(11)	106.9(10)	106.6	106.6	106.8
∠C(10)–Si(4)–H(15)	106.7(8)	106.9	107.8	107.7
ϕH(14)–Si(2)–C(1)–Si(4)	−74.9(21)	−71.5	−75.7	−74.6
ϕH(15)–Si(4)–C(1)–Si(2)	161.6(5)	162.1	163.4	161.6
ϕH(55)–Si(43)–C(42)–Si(44)	46.6(26)	49.6	47.0	47.5
ϕH(57)–Si(44)–C(42)–Si(43)	46.4(16)	47.7	46.1	46.6
ϕH(56)–Si(45)–C(42)–Si(46)	39.4(10)	39.6	40.1	39.4
ϕH(58)–Si(46)–C(42)–Si(45)	−79.8(11)	−79.5	−78.9	−79.7
ϕH(96)–Si(84)–C(83)–Si(85)	39.6(29)	42.6	39.8	40.3
ϕH(98)–Si(85)–C(83)–Si(84)	45.1(14)	46.3	44.8	45.3
ϕH(97)–Si(86)–C(83)–Si(87)	159.9(11)	159.7	160.8	160.0
ϕH(99)–Si(87)–C(83)–Si(86)	−75.9(8)	−75.2	−75.9	−75.9
ϕH(137)–Si(125)–C(124)–Si(126)	46.8(6)	47.4	46.9	46.9
ϕH(139)–Si(126)–C(124)–Si(125)	41.9(11)	41.8	42.4	41.9
ϕH(138)–Si(127)–C(124)–Si(128)	40.8(19)	41.6	40.5	41.0
ϕH(140)–Si(128)–C(124)–Si(127)	161.6(13)	162.6	161.7	161.7
ϕH(178)–Si(166)–C(165)–Si(168)	−76.8(15)	−74.7	−75.7	−76.3
ϕH(219)–Si(207)–C(206)–Si(208)	41.0(32)	44.2	41.3	42.0
ϕH(221)–Si(208)–C(206)–Si(207)	162.0(23)	164.1	161.6	162.2
ϕH(220)–Si(209)–C(206)–Si(210)	41.6(17)	40.7	42.5	41.7
ϕH(222)–Si(210)–C(206)–Si(209)	−81.5(16)	−80.5	−80.2	−81.3
ϕH(260)–Si(248)–C(247)–Si(249)	42.7(12)	43.2	43.6	42.8
ϕH(262)–Si(249)–C(247)–Si(248)	160.6(12)	161.5	160.3	160.6
ϕH(261)–Si(250)–C(247)–Si(251)	−77.1(7)	−76.5	−76.9	−77.1
ϕH(263)–Si(251)–C(247)–Si(250)	37.2(15)	36.9	38.1	37.3
ϕH(301)–Si(289)–C(288)–Si(290)	37.2(19)	36.8	38.4	37.3
ϕH(303)–Si(290)–C(288)–Si(289)	164.9(16)	166.1	164.9	165.0
ϕH(342)–Si(330)–C(329)–Si(332)	−76.9(8)	−76.3	−76.9	−76.9
ϕH(344)–Si(332)–C(329)–Si(330)	39.7(12)	39.8	40.6	39.8

[a] Distances (*r*) are in pm, angles (∠) and dihedral angles (ϕ) are in degrees. Atom numbering is given in Fig. 1. r_e values were calculated using the aug-cc-pVDZ basis set for each respective theory. The estimated standard deviations shown in parentheses represent 1σ.

for bonded distances, but predict angles that lie further from experiment. The experimentally determined dihedral angles are consistently closer to MP2 values than for the other two levels of theory, and MP2 provides overall the best prediction of the structure.

For **1**, MP2 consistently overestimates bonded distances, though by less than 1 %, with the largest discrepancy for the C(1)–Si(2/3/4/5) distance. For this species it is notable that the experimental data show no significant variations between the C(1)–Si(2/3/4/5) distances and those in the HMe_2Si groups. For **2**, **3**, and **4** theory shows slight variations between the C–Si bond lengths in these different environments, with the difference increasing with the size of atom X.

For **2**, **3** and **4** bonded distances, angles, and dihedral angles calculated at the MP2 level were more consistently in agreement with experimental values than were the M06-2X and B3LYP levels of theory. The only exception to this occurs for bonded distances and bond angles to atom X. All levels of theory considerably overestimate these distances, and show variations in angles from experimental by as much as 4°. These deviations from the experimental values are due to insufficiently large basis sets to fully describe these atoms

Table 3. Selected experimental (r_{h1}) and quantum-chemically calculated (r_e) geometric parameters for **2**[a].

Parameter	r_{h1}	r_e B3LYP	r_e M06-2X	r_e MP2
*r*C(1)–Si(2)	189.3(2)	190.9	187.9	189.6
*r*Si(2)–C(12)	186.5(2)	187.9	186.6	187.7
*r*Si(2)–F(14)	160.6(1)	167.5	166.4	167.9
∠Si(2)–C(1)–Si(3)	109.5(3)	108.9	108.6	108.7
∠C(1)–Si(2)–C(12)	116.1(10)	116.4	115.2	115.6
∠C(1)–Si(2)–C(13)	112.9(12)	115.7	113.7	114.1
∠C(1)–Si(2)–F(14)	104.9(6)	104.3	104.6	104.7
∠C(10)–Si(4)–C(11)	109.1(10)	108.9	110.6	110.6
∠C(10)–Si(4)–F(15)	107.3(7)	105.7	107.1	106.8
ϕF(14)–Si(2)–C(1)–Si(3)	81.9(39)	79.7	83.8	83.2
ϕF(16)–Si(3)–C(1)–Si(2)	−167.2(10)	−166.4	−167.4	−167.2
ϕF(15)–Si(4)–C(1)–Si(2)	−153.2(20)	−151.3	−152.1	−152.4
ϕF(17)–Si(5)–C(1)–Si(2)	−39.2(29)	−40.8	−38.2	−39.4
ϕF(55)–Si(43)–C(42)–Si(44)	84.7(26)	86.4	85.3	85.8
ϕF(57)–Si(44)–C(42)–Si(43)	−40.9(33)	−41.4	−39.9	−40.2
ϕF(56)–Si(45)–C(42)–Si(43)	−166.0(46)	−166.4	−165.9	−166.1
ϕF(58)–Si(46)–C(42)–Si(43)	71.2(46)	71.5	72.7	71.9
ϕF(96)–Si(84)–C(83)–Si(85)	77.7(62)	73.4	80.0	79.8
ϕF(98)–Si(85)–C(83)–Si(84)	−163.8(46)	−162.2	−167.0	−163.8
ϕF(137)–Si(125)–C(124)–Si(126)	84.8(26)	87.3	87.2	85.7
ϕF(139)–Si(126)–C(124)–Si(125)	−41.9(17)	−42.2	−41.3	−41.3
ϕF(178)–Si(166)–C(165)–Si(167)	77.9(63)	73.4	79.3	77.3
ϕF(180)–Si(167)–C(165)–Si(166)	73.4(14)	74.0	72.9	73.4
ϕF(219)–Si(207)–C(206)–Si(208)	81.5(19)	80.5	82.5	81.7
ϕF(221)–Si(208)–C(206)–Si(207)	−170.6(23)	−170.1	−171.1	−170.7
ϕF(220)–Si(209)–C(206)–Si(207)	80.3(7)	81.1	80.4	80.3
ϕF(222)–Si(210)–C(206)–Si(207)	−36.7(23)	−38.7	−36.3	−36.8
ϕF(260)–Si(248)–C(247)–Si(249)	80.5(24)	78.1	80.5	80.6
ϕF(262)–Si(249)–C(247)–Si(248)	−161.8(20)	−161.5	−161.5	−161.7
ϕF(261)–Si(250)–C(247)–Si(248)	−157.6(25)	−157.4	−156.7	−157.5
ϕF(263)–Si(251)–C(247)–Si(248)	71.4(38)	71.5	71.6	71.4

[a] Distances (*r*) are in pm, angles (∠) and dihedral angles (ϕ) are in degrees. Atom numbering is given in Fig. 1. r_e values were calculated using the aug-cc-pVDZ basis set for each respective theory. The estimated standard deviations shown in parentheses represent 1σ.

Table 4. Selected experimental (r_{h1}) and quantum-chemically calculated (r_e) geometric parameters for **3**[a].

Parameter	r_{h1}	r_e B3LYP	r_e M06-2X	r_e MP2
*r*C(1)–Si(2)	192.0(4)	194.1	191.1	191.9
*r*Si(2)–C(12)	189.1(4)	188.0	186.9	187.9
*r*Si(2)–Cl(14)	209.1(2)	215.5	213.8	214.4
∠Si(2)–C(1)–Si(3)	110.3(4)	109.4	109.6	109.6
∠C(1)–Si(2)–C(12)	115.3(4)	116.8	116.7	116.4
∠C(1)–Si(2)–C(13)	113.8(4)	115.2	114.5	114.8
∠C(1)–Si(2)–Cl(14)	107.4(5)	107.6	106.8	106.2
∠C(10)–Si(4)–C(11)	107.0(20)	108.4	109.3	109.1
∠C(10)–Si(4)–Cl(15)	107.0(8)	104.1	104.6	104.7
ϕCl(14)–Si(2)–C(1)–Si(3)	39.9(4)	40.2	40.1	40.2
ϕCl(16)–Si(3)–C(1)–Si(2)	159.1(5)	159.2	159.3	159.4
ϕCl(15)–Si(4)–C(1)–Si(2)	−74.9(11)	−73.3	−73.1	−73.5
ϕCl(17)–Si(5)–C(1)–Si(2)	34.7(5)	35.9	35.8	35.8
ϕCl(56)–Si(45)–C(42)–Si(46)	−75.3(6)	−75.0	−74.7	−75.1
ϕCl(58)–Si(46)–C(42)–Si(44)	165.2(7)	165.6	165.8	165.6

[a] Distances (*r*) are in pm, angles (∠) and dihedral angles (ϕ) are in degrees. Atom numbering is given in Fig. 1. r_e values were calculated using the aug-cc-pVDZ basis set for each respective theory. The estimated standard deviations shown in parentheses represent 1σ.

Table 5. Selected experimental (r_{h1}) and theoretical (r_e) geometric parameters for **4**[a].

Parameter	r_{h1}	r_e B3LYP	r_e M06-2X	r_e MP2
*r*C(1)–Si(2)	191.1(5)	194.9	191.9	192.2
*r*Si(2)–C(12)	186.2(3)	188.3	187.1	188.0
*r*Si(2)–Br(14)	227.6(1)	231.6	230.8	230.0
∠Si(2)–C(1)–Si(3)	108.4(2)	109.2	109.4	109.4
∠C(1)–Si(2)–C(12)	118.3(5)	116.4	116.7	116.8
∠C(1)–Si(2)–C(13)	116.4(5)	114.9	114.4	114.8
∠C(1)–Si(2)–Br(14)	107.6(3)	109.8	108.7	107.2
∠C(10)–Si(4)–C(11)	109.0(10)	108.3	109.2	109.1
∠C(10)–Si(4)–Br(15)	102.2(3)	103.5	104.0	104.1
ϕBr(14)–Si(2)–C(1)–Si(3)	39.6(8)	40.4	40.2	39.5
ϕBr(16)–Si(3)–C(1)–Si(2)	158.7(6)	159.2	159.3	158.7
ϕBr(15)–Si(4)–C(1)–Si(2)	−72.7(11)	−73.3	−72.6	−72.9
ϕBr(17)–Si(5)–C(1)–Si(2)	35.0(14)	36.4	35.6	34.8
ϕBr(55)–Si(43)–C(42)–Si(45)	−80.6(11)	−80.5	−81.3	−81.2
ϕBr(56)–Si(45)–C(42)–Si(43)	166.4(8)	166.3	166.4	166.3

[a] Distances (*r*) are in pm, angles (∠) and dihedral angles (ϕ) are in degrees. Atom numbering is given in Fig. 1. r_e values were calculated using the aug-cc-pVDZ(-PP) basis set for each respective theory. The estimated standard deviations shown in parentheses represent 1σ.

(restrictions in available computational time made this necessary). This is further justified below.

For species **2**–**4** the increasing size of the halogen atom leads to the basis sets being used becoming insufficient for full descriptions. Table 6 shows the change in Si–Cl bond length upon moving from the aug-cc-pVDZ through to the aug-cc-pV5Z basis set when calculating the structure of the much simpler H_3SiCl molecule. In order to achieve this set of calculations the level of theory used was also limited to HF. These calculations show clearly that lack of basis set convergence must be at least part of the cause of the deviations between experiment and theory described earlier.

Studies of similar compounds {$(Me_2HSi)_3CSiH_3$ [34] and $(Me_3Si)_3CSiCl_3$ [35]} have been carried out using GED, and comparisons can be drawn with the structures presented in this paper. All four species from this work, plus the two literature studies, have Si–C bonds in common. The C(1)–Si(2/3/4/5) bonds present in species **1**–**4** increase in length when the size of atom X increases.

The GED structure of **1** can be directly compared with the structure of $(Me_2HSi)_3CSiH_3$, for which eleven conformers were modelled for the refinement [34]. Both contain Me_2HSi groups, although $(Me_2HSi)_3CSiH_3$ has two distinct types of central C–Si distances (those to the Me_2HSi groups, and that to SiH_3), with these distances having values of approximately 190 and 188 pm, respectively. Unsurprisingly, the C(1)–Si(2) distance for **1** [189.4(4) pm] agrees well with those determined for the Me_2HSi groups in $(Me_2HSi)_3CSiH_3$ [34]. In that species the angles between two silicon atoms connected through the central carbon take values between 108.1 and 111.7° depending on the orientation of the arms. For **1** the comparable angle [Si(2)–C(1)–Si(3)] is at the lower end of this range (108.3°) as the lack of a smaller SiH_3 substituent in **1** precludes the larger angles for steric reasons.

Molecule **3** from this study can be compared with $(Me_3Si)_3CSiCl_3$ in the literature [35], as both display chlorinated substituents, albeit in different environments. Despite similarities between the Me_3Si substituents in that species and Me_2ClSi in **3**, the lack of the halogen atoms bonded directly to the central carbon atom does alter the chemical environment. The central C–Si distance to the $SiCl_3$ substituent in $(Me_3Si)_3CSiCl_3$ is 189.1(8) pm, while the central C–Si distance in **3** is very similar at 189.1(4) pm. In $(Me_3Si)_3CSiCl_3$ both the central C–Si distance for the trimethylsilyl arms, 191.4(8) pm, and the Si–C distance to the methyl groups, 187.8(6) pm, are shorter than their comparable bonds in **3**, at 192.0(4) and 189.1(4) pm, respectively. This can be explained by the

Table 6. Comparison of Si–Cl bond lengths in H_3SiCl calculated using HF theory with increasing basis set size[a].

Parameter	aug-cc-pVDZ	aug-cc-pVTZ	aug-cc-pVQZ	aug-cc-pV5Z
*r*Si–Cl	209.6	206.9	206.3	205.9

[a] Distances (*r*) are in pm.

lack of electron-withdrawing halogen atoms, which act to weaken the other bonds to silicon. The Si–Cl distance in the $SiCl_3$ group is also shorter than that in the Me_2ClSi group in **3** by almost 6 pm. This is presumably due to the accumulative electron-withdrawing effect of three chlorine atoms drawing more electron density towards themselves.

Within the molecules studied here a noticeable difference can be found when contrasting the central C–Si distances with the silicon-to-methyl carbon distances. The electron- withdrawing nature of the halogen atoms in **2**–**4** cause disparity between these distances within the molecule, with the largest difference found in the Br derivative. This compares favourably with the study of $(XMe_2Si)_2C(SiMe_3)_2$ (X = H, Cl, Br) [36], where the central C–Si distance is consistently longer than that of the methyl carbon to the silicon distance when X = Cl, Br.

Solution-phase dynamic structures

The ^{1}H NMR spectrum of $C(SiBrMe_2)_4$ (**4**) shows, as would be expected, a single broad resonance at room temperature (see Fig. S9 in the Supporting Information). However, on lowering the temperature a much more complicated spectrum emerges (Fig. S9), and at 213 K the spectrum (see Fig. 4) is consistent with the presence of two different conformers. Four smaller peaks (α, β, γ, and δ) may be assigned to a C_2 conformer, and the eight larger peaks (A–H) are commensurate with the eight different methyl-group proton environments associated with a C_1-symmetric conformer. Integration of all signals leads to the conclusion that the C_1 conformer is the most abundant and makes up *ca.* 85 % of the conformer mixture, while the C_2 conformer gives rise to the remaining 15 % of the conformer mixture. Similarly, the ^{29}Si{^{1}H} NMR spectrum is a singlet at room temperature but at low temperature the spectrum (see Fig. 4) shows two smaller signals (1 and 2) associated with the C_2 conformer ^{1}H signals, and four larger signals (I–IV) associated with the C_1-symmetric conformer. Full details of the multinuclear NMR studies of the $C(SiXMe_2)_4$ (X = H, Cl, Br, I) compounds are provided in the Supporting Information.

The ^{1}H and ^{29}Si{^{1}H} NMR spectra for $C(SiClMe_2)_4$ (**3**), show similar, though less well resolved, features to the spectra for the analogous bromide (**4**). Again, sharp singlets at room temperature give rise to much more complicated spectra at low temperature (see Fig. S5) that are consistent with the presence of a less abundant C_2 and a more abundant C_1 conformer, as shown in Fig. 5. The conformers are labelled as for Fig. 4.

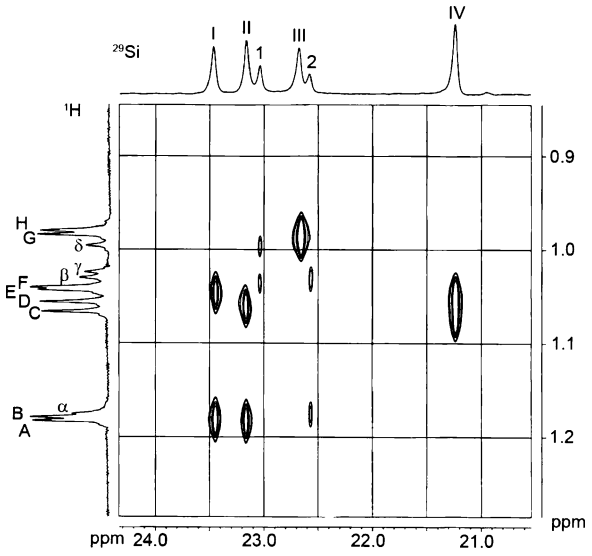

Fig. 4. 2D ^{1}H/^{29}Si NMR correlation spectrum of $C(SiBrMe_2)_4$ (**4**) in $CDCl_3/CD_2Cl_2$ at 213 K. The labelling scheme is explained in detail in the Supporting Information.

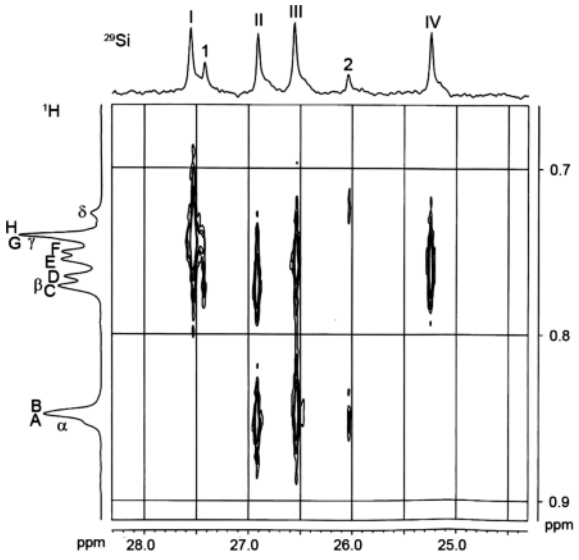

Fig. 5. 2D ^{1}H/^{29}Si NMR shift correlation spectrum of $C(SiClMe_2)_4$ (**3**) in $CDCl_3/CD_2Cl_2$ at 201 K. The labelling scheme is explained in detail in the Supporting Information.

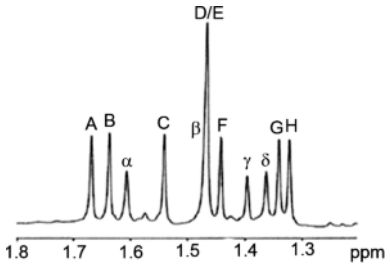

Fig. 6. 360 MHz ^{1}H NMR spectrum of $C(SiIMe_2)_4$ (**5**) at 223 K. The labelling scheme is explained in detail in the Supporting Information.

The NMR studies agree well with the single-molecule *ab initio* calculations showing the two lowest energy conformations possessing C_1 and C_2 symmetry, with the relative proportions of the two conformers at the temperature of experiment being *ca.* 82 and 18 % for the C_1 and C_2 conformer, respectively. Such proportions were also used to fit the GED data and, despite GED being performed in the gas phase rather than in solution, the similarities in relative abundances are not unexpected.

Although it was not possible to determine the gas-phase structure of $C(SiIMe_2)_4$ (**5**), the solution ^{1}H NMR spectrum has been investigated. The ^{1}H NMR spectrum for **5** shows a broad signal at room temperature which, on lowering the temperature, rapidly splits into twelve signals as shown in Fig. 6. This spectrum shows two sets of peaks (A–H) and (α–δ), as did the spectra for the analogous chlorine and bromine compounds, and it is thus reasonable to assume that similar C_1 and C_2 conformers are present for the iodide as well. Further details of the NMR spectra including saturation transfer experiments are given in the Supporting Information (Figs. S13 and S14).

The ^{1}H and ^{29}Si NMR spectra of the much less bulky $C(SiHMe_2)_4$ showed no significant changes when recorded over the range of 333 to 213 K, and no evidence for restricted rotation or the presence of different conformers was observed. For details see the Supporting Information.

Supporting information

Additional details relating to the GED experiments (Table S1); energies relating to all calculated conformers for each species (Tables S2 – 4); details from the GED models and refinements (Tables S5 – 8), amplitudes of vibration and curvilinear distance corrections (Tables S9 – 12); least-squares correlation matrices (Tables S13 – 16); final GED coordinates (Tables S17 – 20); calculated coordinates and energies (Tables S21 – 24); plots of molecular-scattering intensity curves and corresponding radial distribution curves (Figs. S1 – 4); details of NMR spectroscopic studies (Tables S25 – 27; Figs. S5 – 16). This material (337 pages) is available online: DOI: 10.5560/ZNB.2014-4147.

Acknowledgement

We thank the EPSRC for funding the electron diffraction research (EP/C513649 and EP/I004122), for partially funding, with the Chemistry Department, Imperial College, a studentship for K. B., and for funding a studentship for S. Y. (additional funding has come from the School of Chemistry, University of Edinburgh, and the Department of Chemistry, University of York). The authors also wish to thank Dr. A. J. P. White (Imperial College) for the single-crystal X-ray crystallographic studies. We acknowledge the use of the EPSRC U. K. National Service for Computational Chemistry Software (NSCCS) hosted at Imperial College in carrying out this work, which also made use of the resources provided by the Edinburgh Compute and Data Facility (http://www.ecdf.ed.ac.uk/), which is partially supported by the eDIKT initiative (http://www.edikt.org.uk).

[1] C. Eaborn, *J. Chem. Soc., Dalton Trans.* **2001**, 3397.
[2] C. Eaborn, J. D. Smith, *J. Chem. Soc., Dalton Trans.* **2001**, 1541.
[3] P. D. Lickiss in *Comprehensive Organic Functional Group Transformations*, Vol. 6, (Eds.: A. R. Katritzky, O. Meth-Cohn, C. W. Rees), Pergamon, Oxford, **1995**, p. 377.
[4] P. D. Lickiss in *Comprehensive Organic Functional Group Transformations II*, Vol. 6, (Eds.: A. R. Katritzky, R. J. K. Taylor), Elsevier, Oxford, **2005**, p. 381.
[5] R. L. Merker, M. J. Scott, *J. Org. Chem.* **1964**, *29*, 953.
[6] C. Eaborn, P. D. Lickiss, *J. Organomet. Chem.* **1985**, *294*, 305.
[7] A. Kowalewska, P. D. Lickiss, R. Lucas, W. A. Stańczyk, *J. Organomet. Chem.* **2000**, *597*, 111.
[8] P. Kulpinski, P. D. Lickiss, W. A. Stańczyk, *Bull. Pol. Acad. Sci. Chem.* **1992**, *40*, 21.
[9] S.-L. Liu, M.-M. Ma, *J. Organomet. Chem.* **1970**, *24*, 89.

[10] C. Eaborn, A. I. Mansour, *J. Chem. Soc., Perkin Trans. 2* **1985**, 729.
[11] A. I. Al-Mansour, S. S. Al-Showiman, I. M. Al-Najjar, *Inorg. Chim. Acta* **1987**, *134*, 275.
[12] C. Eaborn, P. B. Hitchcock, P. D. Lickiss, *J. Organomet. Chem.* **1984**, *264*, 119.
[13] S. S. Al-Juaid, C. Eaborn, P. B. Hitchcock, P. D. Lickiss, *J. Organomet. Chem.* **1988**, *353*, 297.
[14] R. L. Merker, M. J. Scott, *J. Org. Chem.* **1963**, *28*, 2717.
[15] A. Kowalewska, W. A. Stańczyk, R. Eckberg, *Appl. Catal. A* **2005**, *287*, 54.
[16] M. Ishikawa, M. Kumada, H. Sakurai, *J. Organomet. Chem.* **1970**, *23*, 63.
[17] H. Sakurai, T. Watanabe, M. Kumada, *J. Organomet. Chem.* **1967**, *9*, 11.
[18] X. J. Helluy, J. Kümmerlen, A. Sebald, *Organometallics* **1998**, *17*, 5003.
[19] A. E. Aliev, K. D. M. Harris, D. C. Apperley, R. K. Harris, *J. Solid State Chem.* **1994**, *110*, 314.
[20] A. E. Aliev, K. D. M. Harris, *Mendeleev Commun.* **1993**, 153.
[21] B. Wrackmeyer, H. Zhou, *Spectrochim. Acta A* **1991**, *47*, 849.
[22] J. M. Dereppe, J. H. Magill, *J. Phys. Chem.* **1972**, *76*, 4037.
[23] H. W. Lerner, M. Bolte, *Acta Crystallogr. E* **2005**, *61*, o2326.
[24] R. E. Dinnebier, S. Carlson, S. van Smaalen, *Acta Crystallogr. B* **2000**, *56*, 310.
[25] R. E. Dinnebier, W. A. Dollase, X. Helluy, J. Kümmerlen, A. Sebald, M. U. Schmidt, S. Pagola, P. W. Stephens, S. van Smaalen, *Acta Crystallogr. B* **1999**, *55*, 1014.
[26] B. Beagley, R. G. Pritchard, J. O. Titiloye, *J. Mol. Struct.* **1989**, *212*, 323.
[27] B. Beagley, R. G. Pritchard, J. O. Titiloye, *J. Mol. Struct.* **1988**, *176*, 81.
[28] D. Iroff, K. Mislow, *J. Am. Chem. Soc.* **1978**, *100*, 2121.
[29] H. Bürger, U. Goetze, W. Sawodny, *Spectrochim. Acta A* **1970**, *26*, 685.
[30] C. Eaborn, P. B. Hitchcock, P. D. Lickiss, A. Pidcock, K. D. Safa, *J. Chem. Soc., Dalton Trans.* **1984**, 2015.
[31] A. G. Avent, P. D. Lickiss, A. Pidcock, *J. Organomet. Chem.* **1988**, *341*, 281.
[32] A. G. Avent, S. G. Bott, J. A. Ladd, P. D. Lickiss, A. Pidcock, *J. Organomet. Chem.* **1992**, *427*, 9.
[33] S. L. Masters, D. W. H. Rankin, D. B. Cordes, K. Bätz, P. D. Lickiss, N. M. Boag, A. D. Redhouse, S. M. Whittaker, *Dalton Trans.* **2010**, *39*, 9353.
[34] C. A. Morrison, D. W. H. Rankin, H. E. Robertson, P. D. Lickiss, P. C. Masangane, *J. Chem. Soc., Dalton Trans.* **1999**, 2293.
[35] D. G. Anderson, D. W. H. Rankin, H. E. Robertson, A. H. Cowley, M. Pakulski, *J. Mol. Struct.* **1989**, *196*, 21.
[36] D. A. Wann, M. S. Robinson, K. Bätz, S. L. Masters, A. G. Avent, P. D. Lickiss, manuscript in preparation.
[37] M. J. Frisch, G. W. Trucks, H. B. Schlegel, G. E. Scuseria, M. A. Robb, J. R. Cheeseman, G. Scalmani, V. Barone, B. Mennucci, G. A. Petersson, H. Nakatsuji, M. Caricato, X. Li, H. P. Hratchian, A. F. Izmaylov, J. Bloino, G. Zheng, J. L. Sonnenberg, M. Hada, M. Ehara, K. Toyota, R. Fukuda, J. Hasegawa, M. Ishida, T. Nakajima, Y. Honda, O. Kitao, H. Nakai, T. Vreven, J. A. Montgomery, Jr., J. E. Peralta, F. Ogliaro, M. Bearpark, J. J. Heyd, E. Brothers, K. N. Kudin, V. N. Staroverov, R. Kobayashi, J. Normand, K. Raghavachari, A. Rendell, J. C. Burant, S. S. Iyengar, J. Tomasi, M. Cossi, N. Rega, J. M. Millam, M. Klene, J. E. Knox, J. B. Cross, V. Bakken, C. Adamo, J. Jaramillo, R. Gomperts, R. E. Stratmann, O. Yazyev, A. J. Austin, R. Cammi, C. Pomelli, J. W. Ochterski, R. L. Martin, K. Morokuma, V. G. Zakrzewski, G. A. Voth, P. Salvador, J. J. Dannenberg, S. Dapprich, A. D. Daniels, Ö. Farkas, J. B. Foresman, J. V. Ortiz, J. Cioslowski, D. J. Fox, GAUSSIAN 09 (revision A.1), Gaussian, Inc., Wallingford CT (USA) **2009**.
[38] Edinburgh Compute and Data Facility (ECDF); http://www.ecdf.ed.ac.uk/.
[39] EPSRC-funded NSCCS; http://www.nsccs.ac.uk/.
[40] A. Becke, *J. Chem. Phys.* **1993**, *98*, 5648.
[41] C. Lee, W. Yang, R. Parr, *Phys. Rev. B* **1988**, *37*, 785.
[42] B. Miehlich, A. Savin, H. Stoll, H. Preuss, *Chem. Phys. Lett.* **1989**, *157*, 200.
[43] Y. Zhao, D. G. Truhlar, *Theor. Chem. Acc.* **2008**, *120*, 215.
[44] J. Binkley, J. A. Pople, W. J. Hehre, *J. Am. Chem. Soc.* **1980**, *102*, 939.
[45] M. Gordon, J. Binkley, J. A. Pople, W. J. Pietro, W. J. Hehre, *J. Am. Chem. Soc.* **1982**, *104*, 2797.
[46] R. Kendall, T. H. Dunning, R. Harrison, *J. Chem. Phys.* **1992**, *96*, 6796.
[47] A. Wilson, T. van Mourik, T. H. Dunning, *J. Mol. Struct.* **1996**, *388*, 339.
[48] D. E. Woon, T. H. Dunning, *J. Chem. Phys.* **1993**, *98*, 1358.
[49] K. A. Peterson, D. Figgen, E. Goll, H. Stoll, M. Dolg, *J. Chem. Phys.* **2003**, *119*, 11113.
[50] C. Møller, M. Plesset, *Phys. Rev.* **1934**, *46*, 618.
[51] V. A. Sipachev, *J. Mol. Struct. (THEOCHEM)* **1985**, *121*, 143.
[52] V. A. Sipachev, *J. Mol. Struct.* **2001**, *567*, 67.
[53] C. M. Huntley, G. S. Laurenson, D. W. H. Rankin, *J. Chem. Soc., Dalton Trans.* **1980**, 954.

[54] H. Fleischer, D. A. Wann, S. L. Hinchley, K. B. Borisenko, J. R. Lewis, R. J. Mawhorter, H. E. Robertson, D. W. H. Rankin, *Dalton Trans.* **2005**, 3221.
[55] S. L. Hinchley, H. E. Robertson, K. B. Borisenko, A. R. Turner, B. F. Johnston, D. W. H. Rankin, M. Ahmadian, J. N. Jones, A. H. Cowley, *Dalton Trans.* **2004**, 2469.
[56] A. W. Ross, M. Fink, R. Hilderbrand in *International Tables for Crystallography*, Vol. C, (Ed.: A. J. C. Wilson), Kluwer Academic Publishers, Dordrecht, **1992**, p. 245.
[57] P. D. Lickiss, D. Phil. Thesis, University of Sussex, Falmer, Brighton, **1983**.
[58] N. W. Mitzel, B. A. Smart, A. J. Blake, H. E. Robertson, D. W. H. Rankin, *J. Phys. Chem.* **1996**, *100*, 9339.
[59] A. J. Blake, P. T. Brain, H. McNab, J. Miller, C. A. Morrison, S. Parsons, D. W. H. Rankin, H. E. Robertson, B. A. Smart, *J. Phys Chem.* **1996**, *100*, 12280.
[60] N. W. Mitzel, D. W. H. Rankin, *Dalton Trans.* **2003**, 3650.
[61] W. C. Hamilton, *Acta Crystallogr.* **1965**, *18*, 502.
[62] S. L. Masters, S. J. Atkinson, M. Hölbling, K. Hassler, *Struct. Chem.* **2013**, *24*, 1201.